

Changes in cloud cover associated with Forbush decreases of galactic cosmic rays

Martin C. Todd

Department of Geography, University College London (UCL), London, England, UK

Dominic R. Kniveton

School of Chemistry, Physics and Environmental Science, University of Sussex, Brighton, England, UK

Abstract. The results of a study to quantify the relationship between cloud cover and short-term Forbush decreases (FD) of galactic cosmic ray flux are presented. Using an extensive record of global satellite-derived cloud products from the International Satellite Cloud Climatology Project (ISCCP) D1 data series, epoch superposition analysis of a sample of FD events is conducted. This analysis is conducted at a range of spatial scales from global, through 5° geomagnetic latitude bands to a global grid with 2.5° resolution. Resulting cloud anomalies are tested for significance using a randomized Monte Carlo experiment. The results indicate a small but significant (at 0.001 probability level) decline in the global proportion of cloud cover (of up to 1.4%) immediately prior to and following FD events. Analysis of data averaged over geomagnetic latitude (φ) bands reveals that significant cloud anomalies are concentrated in the high latitudes. A substantial (small) decline in cloud cover occurs at Southern (Northern) Hemisphere polar latitudes and is accompanied by a small but significant increase near $\varphi = 30^\circ\text{N}$. The high-latitude anomalies occur largely in the high-level cloud and are particularly pronounced (up to -30%) in the uppermost cloud (occurring at 10–180 mbar) over Antarctica. In contrast, analysis using a sample of FD events associated with solar proton events shows no statistically significant cloud anomalies. A discussion of possible explanations of the results is provided.

1. Introduction

There is a long history of solar-climate studies, many of which have shown correlations with high statistical significance between atmospheric parameters and solar variability [e.g., *Labitzke and van Loon*, 1989, 1992; *Lassen and Friis-Christensen*, 1995; *Mason and Tyson*, 1992; *van Loon and Labitzke*, 1998]. Criticism of certain solar-climate studies has focused on the lack of physical explanation of how very low energy fluxes implicit in solar irradiance variations are able to cause observed climate variability involving much higher energy fluxes. However, the question of how and to what extent the climate system may be influenced by solar-related variability remains central to our understanding of any anthropogenic effects on climate. In this context, the studies of *Svensmark and Friis-Christensen* [1997] and *Marsh and Svensmark* [2000] have proved notable in that a statistical relationship between satellite-derived low-level cloudiness and galactic cosmic ray flux (GCR) was demonstrated, at low to middle latitudes over interannual timescales. Such work is significant given the importance of clouds to the Earth's radiation budget [*Ramanathan et al.*, 1989].

GCR is known to vary out of phase with the 11-year solar sunspot cycle and may have exhibited a long-term decline since the nineteenth century [*Feynman and Ruzmaikin*, 1999]. Thus changes in cloud cover associated with GCR variations may result in greater radiative effects than those associated with solar output itself. The work of *Svensmark and Friis-Christensen* [1997] proved controversial, prompting a number of reassessments [*Farrar*, 2000; *Jorgensen and Hansen*, 2000; *Kernthaler et al.*, 1999; *Kristjansson*

and *Kristiansen*, 2000]. These studies raised doubts about the longer-term stability of the cloud-GCR relationship and suggested that the observed variability in cloud cover may be related to internal climate mechanisms of the El Niño-Southern Oscillation and volcanic activity rather than GCR variability. Thus, the possible influence of variability of GCR on cloud cover and the planet's radiation budget has remained one of the more hotly debated issues in climate science in recent years.

Cosmic rays comprise energetic particles, mainly protons, originating from all directions in space, from both solar and nonsolar sources. A distinction can be made between solar protons (SP) with relatively low energy levels (10–300 MeV) and GCR with higher energy levels (300 MeV to 10 GeV). The solar wind has a strong role in modulating cosmic ray intensity [*Yamada et al.*, 1998]. In particular, at short timescales, irregular decreases of GCR intensity, known as Forbush decreases (FD), can be observed. FD events are associated with magnetohydrodynamic disturbances following solar coronal mass ejections [*Krivsky and Ruzickova-Topolova*, 1978; *Reiter*, 1992].

Upon entering the magnetosphere, cosmic ray particles are influenced by the Earth's magnetic field and the configuration of the magnetosphere. As the cosmic ray particles enter the atmosphere, they collide with other atmospheric particles. Cosmic rays are the principle cause of ionization in the lower atmosphere, which peaks at a height of 10–20 km in the atmosphere. It has been suggested that cosmic ray ionization has direct and indirect impacts on cloud microphysics [*Dickinson*, 1975; *Tinsley and Deen*, 1991; *Tinsley et al.*, 1989]. GCR may directly influence cloud through the production, via cosmic ray ionization, of cloud condensation and/or ice nuclei. Indirect mechanisms include modulation of the atmospheric electrical conductivity within the “global electric circuit” by GCR ionization and subsequent effects on cloud microphysics through the process of electro-scavenging [*Tinsley et al.*, 2000]. *Tinsley et al.* [2000] showed greater scav-

enging rates for charged evaporation aerosols in nonthunderstorm clouds compared to noncharged aerosols. A further indirect mechanism has been proposed in which GCR ionization influences nitrous oxide and ozone production and thus stratospheric heating rates. This alters the stratospheric and tropospheric circulation and possibly the cloud distribution [Brasseur and Solomon, 1995]. Through both direct and indirect processes it is hypothesized that an increase (decrease) in GCR should result in an increase (decrease) in cloud, greatest for high clouds and at high geomagnetic latitudes where transmission of the cosmic ray flux is at its maximum. FD events have been associated with a decline in high cloud at high latitudes of the Northern Hemisphere [Pudovkin and Veretenenko, 1995].

However, the magnitude of these direct and indirect GCR/cloud interactions in the atmosphere remains largely unconfirmed [Pruppacher and Klett, 1997]. Additionally, attempts to quantify the effects of GCR on cloud are complicated by variations in other solar related parameters coincident with FD events. SP events may be associated with FD events and may cause ionization higher in the atmosphere than GCR particles, principally at the poles [Brasseur and Solomon, 1995]. Changes in solar irradiance especially at ultraviolet wavelengths have also been linked with the large-scale tropospheric circulation [Haigh, 1996, 1999], which may then affect the distribution of cloud. Solar activity and the electric field of the solar wind itself may also affect the global electric circuit (and thus cloud processes) through generation of enhanced ionospheric cross polar cap voltage [Bezprozvannaya et al., 1997]. There is evidence that such processes modulate the large-scale stratospheric and tropospheric circulation at high latitudes [Tinsley and Heelis, 1993; Bezprozvannaya et al., 1997].

In this context, there is a clear need for observational studies to assess the evidence for the operation of such mechanisms at climate space scales and timescales. The aim of this study is to quantify the effect of short-term Forbush decreases in GCR (in isolation from other solar variables) on global and regional patterns of cloud cover. Utilizing the most comprehensive database of global cloud cover currently available, produced for the International Satellite Cloud Climatology Program (ISCCP), this study is the first to assess any systematic effect of FD events on cloud cover at the global scale.

2. Data and Methods

ISCCP D1 data were obtained for the period 1986 to 1994, representing the full extent of currently available data (although the data will eventually extend from 1983 to the present day). The D1 format provides global estimates of a range of cloud parameters every 3 hours on a 2.5° latitude-longitude grid [Rossow et al., 1996]. The D series algorithms have been modified significantly from the C series algorithm. Modifications include changes to improve the detection of clouds and reduction in bias [Rossow and Schiffer, 1999]. We selected 24 variables representing all the available information on cloud amount, expressed as the proportion of all pixels in a grid cell (Table 1). The cloud classification utilized by ISCCP for variables 10–24 involves a two-dimensional threshold of cloud height and optical depth and as such is dependent on the availability of visible data [Rossow et al., 1996]. These ISCCP D1 data were accumulated over 24-hour periods to remove the effects of diurnal variability in cloud cover.

The methodology adopted here is the “epoch superposition” analysis used in previous studies of this kind. This method is used in many scientific fields to find general patterns in temporal data sets. In this study we have selected a sample of isolated FD events (separated by more than 11 days from another event). These dates (listed in Table 2) represent the onset of FD events (defined by a decline greater than 3%) at the Earth’s surface as recorded by the neutron monitor at Mount Washington, New Hampshire, USA (44.3°N, 288.7°E). In order to quantify precisely the nature of

Table 1. Cloud Variables Extracted From ISCCP D1 Data Used in This Study

Variable	Description
1	proportion of all pixels defined as cloudy
2	proportion of all pixels defined as cloudy (daytime observations only)
3	proportion of all pixels defined as level 1 cloud (10–180mb) ^a
4	proportion of all pixels defined as level 2 cloud (180–310mb) ^a
5	proportion of all pixels defined as level 3 cloud (310–440mb) ^a
6	proportion of all pixels defined as level 4 cloud (440–560mb) ^a
7	proportion of all pixels defined as level 5 cloud (560–680mb) ^a
8	proportion of all pixels defined as level 6 cloud (680–800mb) ^a
9	proportion of all pixels defined as level 7 cloud (800–1000mb) ^a
10	proportion of all pixels defined as cloud type 1 (liquid cumulus) ^b
11	proportion of all pixels defined as cloud type 2 (liquid stratocumulus) ^b
12	proportion of all pixels defined as cloud type 3 (liquid stratus) ^b
13	proportion of all pixels defined as cloud type 4 (ice cumulus) ^b
14	proportion of all pixels defined as cloud type 5 (ice stratocumulus) ^b
15	proportion of all pixels defined as cloud type 6 (ice stratus) ^b
16	proportion of all pixels defined as cloud type 7 (liquid altocumulus) ^b
17	proportion of all pixels defined as cloud type 8 (liquid altostratus) ^b
18	proportion of all pixels defined as cloud type 9 (liquid nimbostratus) ^b
19	proportion of all pixels defined as cloud type 10 (ice altocumulus) ^b
20	proportion of all pixels defined as cloud type 11 (ice altostratus) ^b
21	proportion of all pixels defined as cloud type 12 (ice nimbostratus) ^b
22	proportion of all pixels defined as cloud type 13 (ice cirrus) ^b
23	proportion of all pixels defined as cloud type 14 (ice cirrostratus) ^b
24	proportion of all pixels defined as cloud type 15 (deep convective) ^b

^a Variable is based on thermal IR data only.

^b Variable is dependent on the availability of satellite visible data.

GCR flux during FD events we have also analyzed hourly neutron monitor records at three other sites located at high geomagnetic latitudes: Newark, New Jersey (USA, 39.7°N, 284.2°E), McMurdo (Antarctica, 77.8°S, 166.7°E), and the South Pole (88.0°S, 210.0°E). Over the relatively short period for which we have ISCCP data there are total of 50 FD events. Some of these coincide (within 3 days either side) with SP events. It has been hypothesized that during FD events associated with SP events an increase in ionization (and any effect on cloud) from solar protons is likely to oppose any decrease associated with a decline in GCR. To isolate the GCR signal from that of SP we have distinguished the FD events into separate samples of 23 FD events when no SP event occurs (hereinafter referred to simply as FD events) and 27 coincident FD events coincident with SP events (FD-SP). This has the additional benefit of facilitating a distinction of any GCR signal from other effects associated with solar flares and other phenomena which may also influence cloud, as noted in section 1. The FD-SP events represent a “control sample” of solar proton

Table 2. Onset Dates and Magnitude of Forbush Decreases in Galactic Cosmic Ray Flux (Recorded at Mt. Washington Neutron Monitor) Used in This Study

FD Event	FD Date (Magnitude, %)	FD-SP Date (Magnitude, %)
1	May 4, 1984 (5.3)	April 25, 1985 (6.4)
2	July 3, 1984 (5.5)	February 6, 1986 (9.8)
3	September 12, 1984 (5.7)	March 8, 1986 (3.1)
4	November 3, 1986 (4.1)	January 4, 1988 (4.2)
5	May 24, 1987 (2.6)	August 24, 1988 (4.2)
6	August 24, 1987 (4.9)	October 9, 1988 (3.7)
7	February 20, 1988 (5.1)	December 17, 1988 (4.7)
8	July 20, 1988 (2.5)	January 4, 1989 (5.5)
9	February 11, 1989 (4.4)	March 12, 1989 (15.5)
10	August 19, 1989 (4.0)	March 26, 1989 (3.8)
11	August 28, 1989 (4.9)	August 9, 1989 (3.7)
12	September 18, 1989 (4.2)	September 4, 1989 (7.2)
13	May 17, 1990 (3.9)	October 20, 1989 (13)
14	March 12, 1991 (4.8)	November 17, 1989 (4.2)
15	April 24, 1991 (6.6)	November 28, 1989 (16)
16	August 18, 1991 (5.1)	March 18, 1990 (6.6)
17	November 7, 1991 (5.5)	April 7, 1990 (7.7)
18	February 25, 1992 (7)	January 30, 1991 (3.5)
19	September 8, 1992 (4.5)	March 24, 1991 (23.5)
20	February 19, 1993 (4.8)	May 28, 1991 (7.5)
21	October 22, 1993 (4.9)	June 11, 1991 (11.2)
22	April 16, 1994 (5.0)	June 30, 1991 (7.4)
23	June 17, 1994 (3.0)	July 8, 1991 (5.1)
24		October 27, 1991 (10.7)
25		May 9, 1992 (5.6)
26		October 31, 1992 (3.5)
27		February 20, 1994 (3.4)

events in which the effect of GCR changes may be minimized but not that of other solar related parameters.

For each of these FD and FD-SP events, ISCCP D1 data are extracted for the period from 5 days before to 5 days following each event. The cloud parameters are then averaged over the sample (23 FD and 27 FD-SP events) for each time slot (day -5 to 5) separately. In this way the mean value of any cloud parameter for day n is taken to be representative of the conditions on such days. This is akin to compositing routinely used in climate analysis. The difference between conditions prior to, during, and after FD events can then be established by subtracting the mean values at different time slots. Here we define a “base period” sample representative of conditions prior to an event as the mean of days -5 to -3 . The mean cloud values at all days from day -1 to day 5 are then derived, and from this the anomaly is obtained by subtracting the mean of the base period. The result is tested for local statistical significance using a t-test. Throughout, the anomalies are given as absolute values rather than as a percentage of the base period value.

This analysis is conducted at a range of spatial scales from global averages through 5° geomagnetic latitude bands to every 2.5° grid cell over the globe. Because the actual area of grid cells varies with latitude, it is necessary to ensure that the quantities derived at all scales larger than that of individual cells represent an accurate estimate of the true areal average. Thus cloud proportions at global and latitude band scales are derived from the actual numbers of satellite pixels (total and cloudy) within the entire region rather than by averaging the grid cell cloud proportions.

In the case of the smallest spatial scale (2.5° grid), there are potential problems in interpreting the collective statistical significance of gridded fields of finite numbers of statistical tests such as t-tests. These problems stem from the effects of finite sample size and spatial autocorrelation in global climate data sets [Livezey and Chen, 1983]. To address this problem, the global percentage area (A_e) of locally significant t-tests (on the difference in cloud variables between the base period and a given day -1 to 5) was tested for field significance. This was achieved by undertaking a

randomized Monte Carlo simulation, consisting of 1000 runs, in which the probability density distribution (PDD) of the percent area of locally significant t-tests (at the 0.05 probability level) for random data (A_r) was estimated. In each of the 1000 experimental “runs” a sample of n (equal to that used in the analysis of FD events) “epochs” (a consecutive 11 day period) were randomly drawn from a database of over 2000 days. By comparing A_e with the PDD of A_r , the statistical likelihood that the observed A_e has occurred by chance can be calculated.

3. Results

Figure 1 shows the mean proportion of cloud cover during the base period day -5 to day -3 . The structure of cloud cover is in very close agreement both in terms of absolute and relative cloud amounts with the long-term average cloud conditions determined from the ISCCP D2 data set [Rossow and Schiffer, 1999]. From this we are confident that our sample of events is representative of the long-term climatology, providing evidence that our sample size is large enough to highlight any systematic changes in cloud cover associated with FD events.

Figure 2 shows the composite mean hourly GCR flux recorded at the Newark, McMurdo, and South Pole neutron monitors. Although there is dispersal within the composite mean, the magnitude and duration of FD events are clearly apparent. It is important to note that the decline in GCR at these stations begins about ~ 12 hours prior to 0000 UTC on the FD onset day (day 0) as recorded at the Mt. Washington site and used as the sampling basis in this study.

The mean anomalies of globally averaged values of all cloud variables at days -1 to 5 during FD events are presented in Table 3. There are statistically significant declines in the proportion of total cloud and level 1–3 cloud. There is a clear pattern of reduced cloud cover from day -1 , with a minimum at day 1, when the absolute cloud proportion falls from 0.64 during the base period to 0.626, an anomaly of -0.014 or 1.4% (Figure 3 and Table 3). This is then followed by a rise to day 5. Total cloud proportion

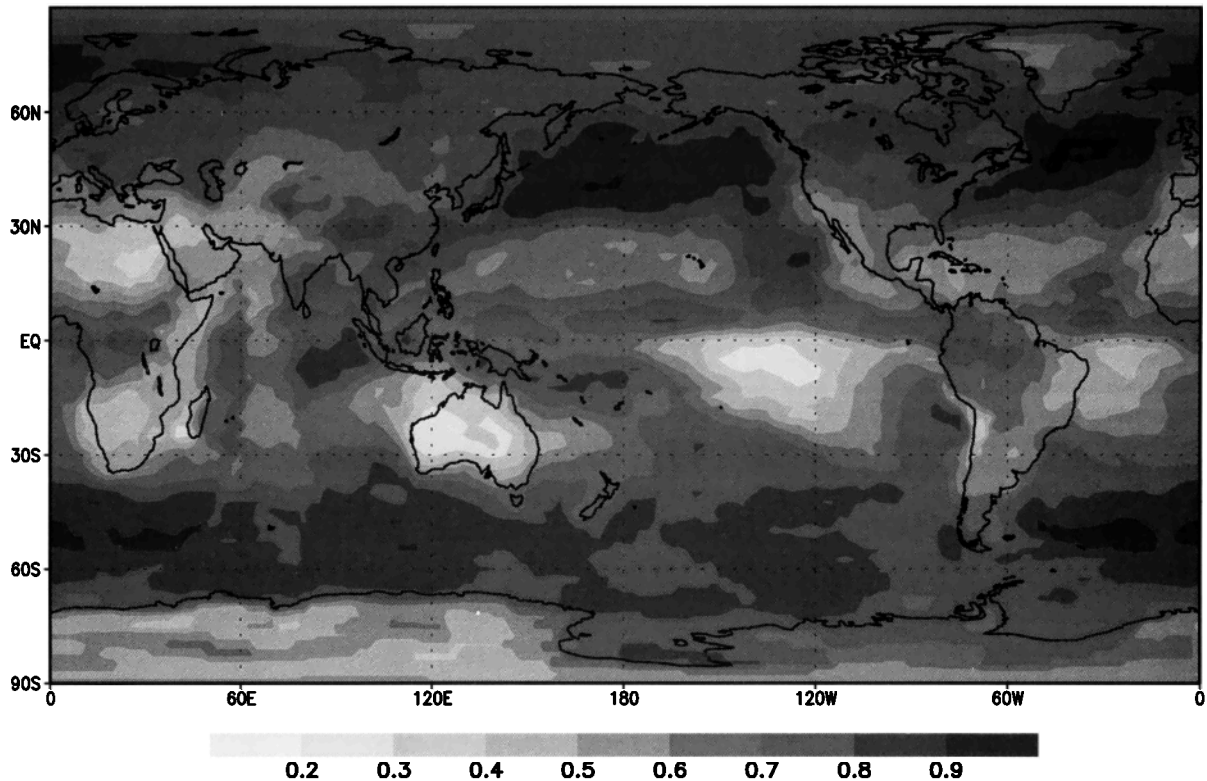


Figure 1. Mean total cloud proportion during the “base period” (days -5 to -3 prior to onset of FD events).

anomalies at day -1 to day 1 are significant at the 0.01 probability level (Table 3). Of particular interest, however, is the precise nature and location of the cloud exhibiting this decline during FD events. Much of the decline in global cloud cover occurs preferentially over land surfaces, where significant anomalies at 0.01 probability level are observed on days -1 to 1 and at the 0.05 probability level on days 2 and 5. A maximum decline of -0.034 (3.4%) is observed on day 1 (Figure 3). None of the 24 cloud variables

show significant anomalies (even at the 0.1 probability level) on days -1 to 5, over “global” ocean surfaces.

Analysis of cloud proportion anomalies at various levels in the atmosphere (Figure 4 and Table 3) indicates that upper level cloud (levels 1–4) shows a decline throughout the FD event period, while (middle) level 5 cloud tends to increase slightly from day 2 onward (although not significantly). The lowest cloud levels 6 and 7 have insignificant near zero anomalies throughout

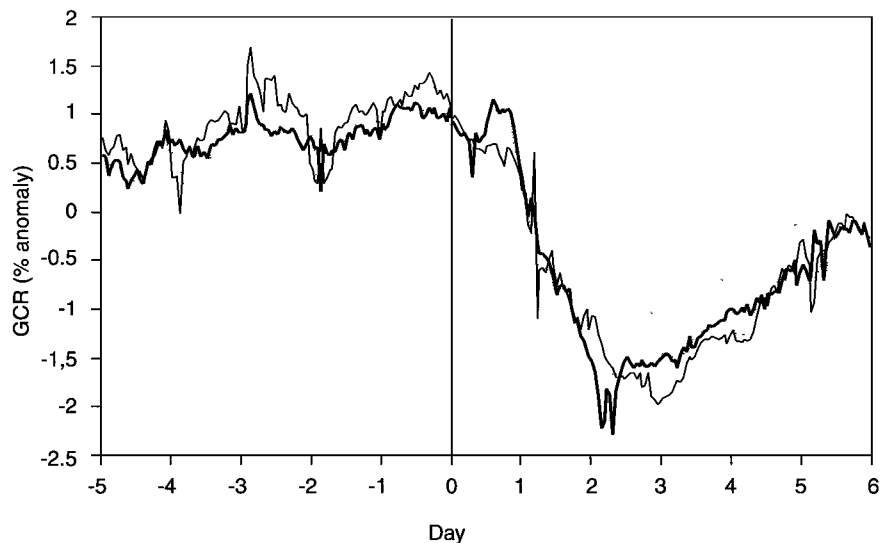


Figure 2. Mean GCR flux anomaly (relative to 11-day period day -5 to day 5) recorded hourly over the period day -5 to day 5 at the Newark (dotted line), McMurdo (thin line), and South Pole (thick line) neutron monitors.

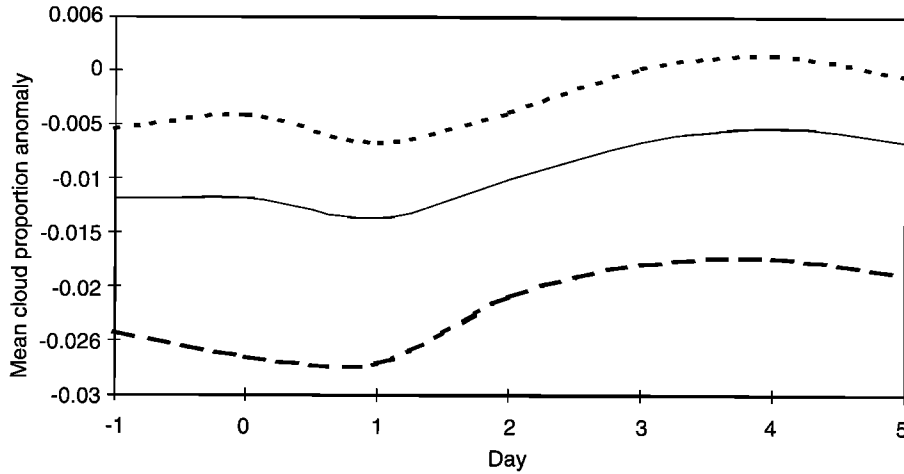


Figure 3. Mean absolute global total cloud proportion anomalies (proportion of total pixels, relative to base period) on days -1 to 5 (thin line), for land regions only (long-dashed line), and for ocean regions only (short-dashed line). See Table 3 (text) for statistical significance of anomalies at global scale (land and sea).

the period (Figure 4 and Table 3). Global anomalies are significant (at the 0.05 probability level) for level 3 cloud on days -1 to 3 , and for level 1 cloud on days 0 and 1 and level 2 cloud on day 3 (at the 0.1 probability level). Thus, although significant anomalies are not observed for all upper level clouds on all days, the general pattern is for negative anomalies for upper level cloud proportion during FD events. The higher significance levels associated with anomalies in total cloud proportion rather than individual cloud levels indicate that total cloud cover reductions are the cumulative effect of consistent reductions in high-level cloud (levels 1–4).

In terms of the magnitude of the change in total cloud cover it is the highest-level cloud that is most important. Of the global decline of -0.014 in cloud proportion at day 1 , the contributions from cloud levels 1–4 are -0.0043 , -0.0028 , -0.0033 , and -0.0022 , respectively (Table 3). The equivalent figures for land surfaces where the “global” decline is -0.034 are -0.015 , -0.007 , -0.008 , and -0.004 . That low-level cloud (levels 5–7) generally shows slight (but insignificant) increases during FD events may be a result of the “top down” viewing characteristics of the satellites in conditions where there is less higher-level cloud, rather than a real increase in low cloud.

Table 3. Global Mean Values For Base Period (Day -5 to Day -3) and Absolute Anomalies (Relative to Base Period) Associated With FD Events, for All Cloud Variables^a

Variable	Base Period Mean	Day -1	Day 0	Day 1	Day 2	Day 3	Day 4	Day 5
1	0.63979	(-0.01201) ^b	(-0.01189) ^b	(-0.01363) ^b	(-0.00995) ^c	-0.00648	-0.00514	-0.00656
2	0.64886	-0.00284	-0.00501	-0.00996	-0.0114	-0.00897	-0.00574	-0.00437
3	0.01837	-0.00279	(-0.00412) ^d	(-0.00429) ^d	-0.0037	-0.00189	-0.00255	-0.00212
4	0.04541	-0.00171	-0.00148	-0.00278	-0.00246	-0.004 ^d	-0.0024	-0.00183
5	0.0732	(-0.00335) ^c	(-0.00337) ^d	(-0.00335) ^d	(-0.00383) ^c	(-0.00371) ^c	-0.00254	-0.00259
6	0.09924	-0.00451	-0.00368	-0.00217	-0.00249	-0.00189	-0.00148	-0.00154
7	0.11998	0.0015	0.00011	0.00009	0.00256	0.00351	0.00277	0.00196
8	0.13045	-0.00183	-0.00065	-0.00083	0.00063	0.00069	0.00022	0.00039
9	0.11507	-0.00001	0.00076	-0.00059	0.00076	0.00082	0.00011	-0.00063
10	0.11726	-0.00196	-0.00082	-0.00037	0.00025	0	-0.00038	-0.00044
11	0.14948	-0.00337	-0.00387	-0.00391	-0.00361	-0.00259	-0.00142	-0.00233
12	0.0628	0.00034	0.00099	-0.00141	-0.00127	-0.00068	-0.00137	-0.00277
13	0.06097	-0.00109	-0.00135	0.00184	0.00341	0.00305	0.00314	0.00405
14	0.08178	-0.00585	-0.00623	0.0005	0.00242	-0.00009	-0.00199	0.00231
15	0.0383	-0.00543	-0.00349	-0.00185	-0.00027	-0.00131	-0.00199	-0.00039
16	0.09283	-0.00067	-0.00056	-0.00119	0.00016	0.00029	0.00078	-0.00064
17	0.11197	-0.00255	-0.00391	-0.00384	-0.00324	-0.00338	-0.00333	-0.00292
18	0.05551	-0.00041	-0.00222	-0.00128	-0.00086	0.00029	-0.00069	-0.00253
19	0.06932	-0.00068	-0.00123	-0.00169	0.00034	0.00082	0.00083	-0.00093
20	0.10643	-0.00432	-0.00537	-0.005	-0.00331	-0.00304	-0.00379	-0.00271
21	0.05157	-0.00142	-0.00297	-0.00209	-0.00081	0.00043	-0.00043	-0.00223
22	0.13885	0.00024	0.00191	0.00327	0.00361	0.0015	0.00035	0.00006
23	0.10844	0.00114	-0.00065	-0.00086	0.00062	-0.00014	-0.00038	0.00012
24	0.07452	0.00106	-0.0004	-0.00094	0.00102	0.00177	0.00334	0.00472

^a Significant anomalies (at all levels <0.1) shown in parentheses.

^b Significant anomalies at the 0.01 probability level.

^c Significant anomalies at the 0.05 probability level.

^d Significant anomalies at the 0.1 probability level.

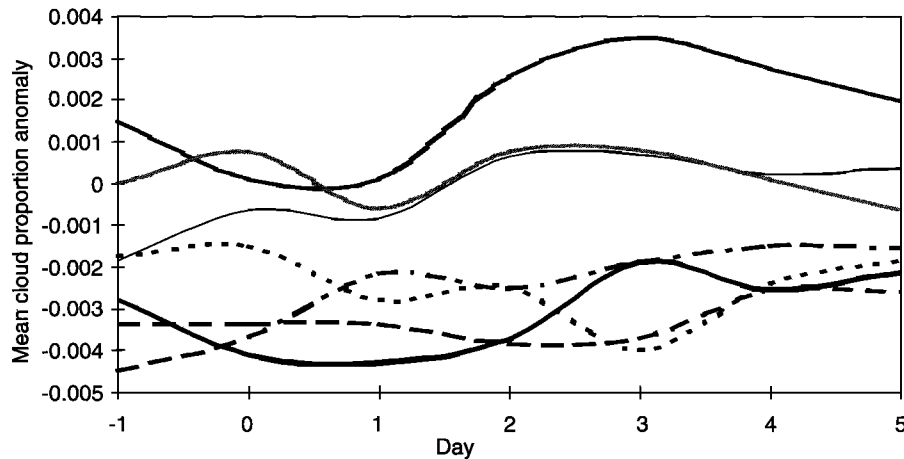


Figure 4. Mean global cloud proportion anomalies (relative to base period) on days -1 to 5 for cloud levels 1 to 7 (thick solid, dotted, dashed, dot-dashed, medium shaded, thin solid, and light shaded, respectively). See Table 3 for statistical significance of observations.

It appears that the largest anomalies may occur at nighttime (and/or during the winter season at high latitudes) since there are no significant anomalies observed using the daytime observations only (Table 3, variable 2), even over land surfaces (not shown). In addition, none of the cloud-type variables derived using the daytime visible data show any significant anomalies (Table 3, variables 10–24). However, this may be a result of larger errors in the ISCCP variables derived from multispectral algorithms.

As described in section 1, much of the theory on the interaction of GCR and cloud suggests a geomagnetic latitudinal (φ) dependence of these processes, because of the strong role the Earth's

magnetic field plays in modulating GCR. Accordingly, cloud anomalies were also derived in 5° φ bands. Significant anomalies (at the 0.05 probability level) in total cloud proportion emerge only in particular locations, dominated by large negative anomalies (up to -0.18 or 18%) over the polar latitudes of the Southern Hemisphere (poleward of $\varphi = 70^\circ\text{S}$) throughout the FD epoch, peaking at day 1 (Figure 5). There are smaller negative anomalies (-0.06 or 6%) over the polar latitudes of the Northern Hemisphere (poleward of $\varphi = 75^\circ\text{N}$) significant only on day 0, and small positive anomalies (up to 0.02 or 2%) near $\varphi = 30^\circ\text{N}$, significant on days 2, 4, and 5.

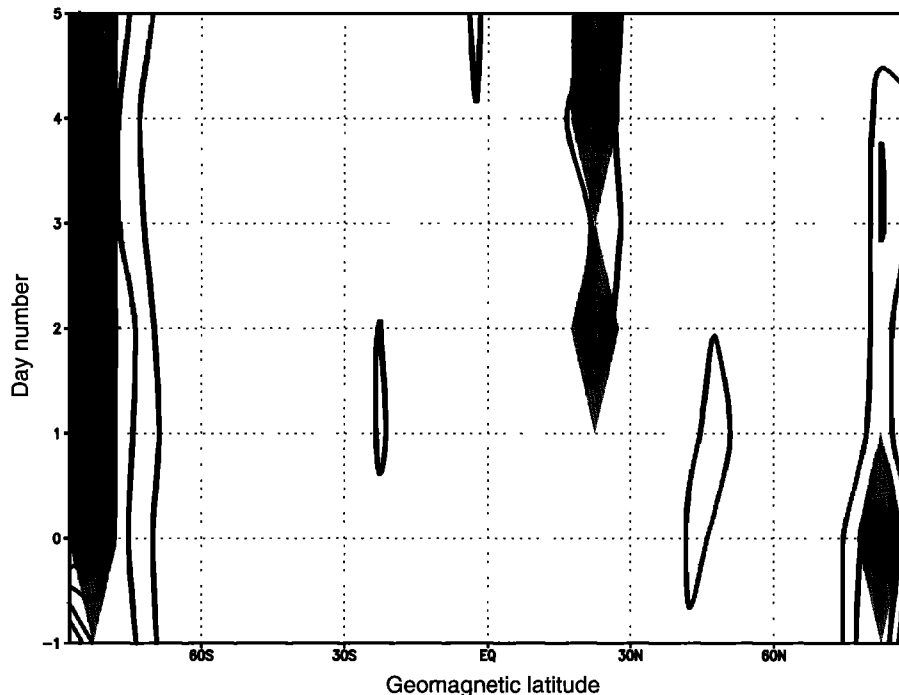


Figure 5. Zonal mean (averaged over 5° geomagnetic latitude bands) total cloud proportion anomalies (relative to base period) for days -1 to 5 . Positive (negative) anomalies have solid (dotted) contours. The contour interval is 0.02, the zero contour is omitted, and statistically significant anomalies (at 0.05 probability level) are shaded.

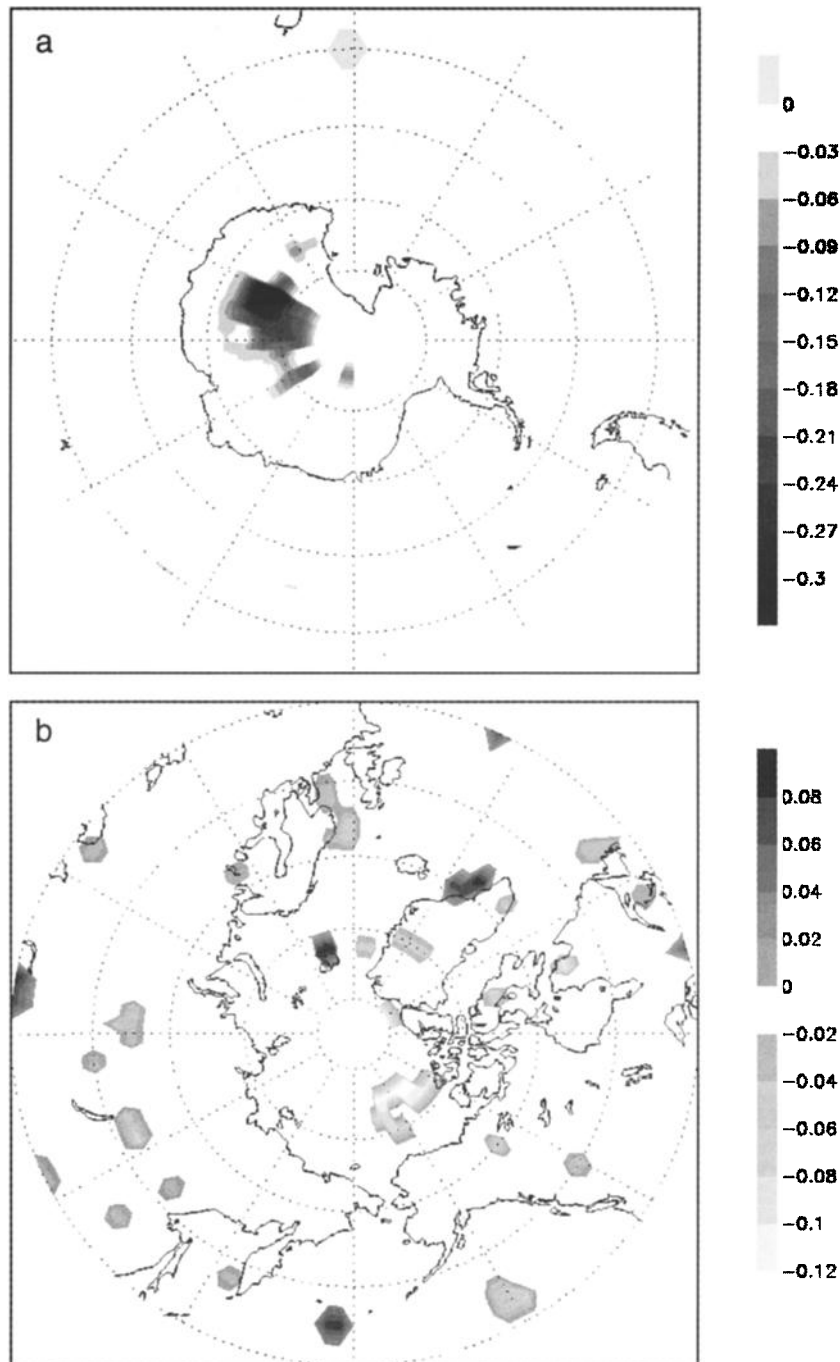


Figure 6. Mean anomalies (relative to base period) on a 2.5° grid for (a) proportion of cloud level 1 (45° – 90° S on day 1) and (b) proportion cloud level 4 (45° – 90° N on day -1). Only locally significant anomalies (at 0.05 probability level) are shown.

Analysis of the individual cloud levels shows that the cloud anomalies in the polar region of the Southern (Northern) Hemisphere are primarily associated with cloud level 1 (4) (not shown). In both cases this is the highest cloud level where any substantial cloud amount occurs in these regions, such that FD events appear to influence the highest cloud in the polar zones. There is no coherent pattern of statistically significant anomalies in low-level clouds (not shown). Interestingly, there is little evidence of significant changes in cloud cover (or any cloud variable including cirrus cloud) in the band $\varphi = 60^\circ - 64^\circ$ N,

where *Pudovkin and Veretenenko* [1995] observe a decline in high-level cloud (from surface observation in the former USSR) following FD events, even when the focus is on winter months only (not shown).

The results of the Monte Carlo simulations to test the field significance of 2.5° gridded fields of cloud anomalies show that only a very few of the variables produce anomaly patterns that are field significant at any useful significance level. This is likely to reflect the high degree of cloud variability apparent at this small scale, associated with the day-to-day mesoscale, synoptic, and

Table 4. Global Mean Values for Base Period (Day -5 to Day -3) and Absolute Anomalies (Relative to Base Period) Associated With FD-SP Events, for All Cloud Variables

Variable	Base Period	Day -1	Day 0	Day 1	Day 2	Day 3	Day 4	Day 5
1	0.63858	-0.00194	-0.00414	-0.00091	-0.00065	-0.00322	-0.00227	-0.00203
2	0.638961	-0.00816	-0.00921	-0.00488	-0.00496	-0.00574	-0.00373	0.001017
3	0.01343	0.00038	0.00034	0.00055	0.00017	0.00182	0.00109	0.00232
4	0.0413	0.00016	-0.00047	0.0004	-0.00019	0.00008	0.00125	0.00266
5	0.06913	-0.00044	-0.00063	0.00077	0.00128	-0.00028	-0.00001	0.00237
6	0.10242	0.0036	0.00394	0.00398	0.00529	0.00196	0.0001	-0.00217
7	0.12645	-0.00077	-0.00075	-0.0029	-0.00412	-0.00342	-0.00235	-0.00412
8	0.13084	-0.00047	-0.00272	-0.00249	-0.00237	-0.00198	-0.00087	-0.00292
9	0.11551	-0.00371	-0.00374	-0.00115	-0.00101	-0.00277	-0.00187	-0.00048
10	0.11585	-0.00166	-0.00118	-0.0007	-0.00077	-0.00099	-0.00141	-0.00176
11	0.14836	-0.00184	-0.00248	-0.0015	-0.00076	-0.0023	-0.00215	-0.00172
12	0.06456	-0.00044	-0.00142	0	-0.00036	0.00253	0.00419	0.00361
13	0.06363	-0.0024	-0.00284	-0.00036	-0.00103	-0.00112	-0.0008	-0.00137
14	0.08429	-0.00398	-0.00307	-0.00129	0.0019	0.00058	0.00065	0.00236
15	0.04474	-0.00177	-0.0018	-0.00046	-0.00008	0.00218	0.00245	0.00109
16	0.09063	-0.00057	-0.00044	-0.00077	-0.00087	-0.00051	-0.001	-0.00193
17	0.11299	-0.00009	-0.0015	-0.00297	-0.00298	-0.00302	-0.00409	-0.00399
18	0.05813	-0.00184	-0.00135	-0.00155	-0.00061	-0.00051	-0.00107	-0.00204
19	0.06627	-0.00021	-0.00096	-0.00184	-0.00216	-0.00245	-0.00243	-0.0025
20	0.11031	0.00086	-0.00212	-0.00402	-0.00422	-0.00574	-0.00658	-0.00503
21	0.05844	-0.00129	-0.00146	-0.00196	-0.00085	-0.00237	-0.00299	-0.00347
22	0.1348	-0.0028	-0.00185	-0.00032	0.0014	0.00128	0.00127	0.00421
23	0.10906	-0.00067	0.00049	0.00136	-0.00079	-0.00026	0.00174	0.00521
24	0.0759	0.00178	0.00059	0.00031	-0.00138	0.0003	0.00237	-0.00024

planetary-scale circulation. However, the few field significant results provide valuable detail which complements the results of the analysis conducted at larger scales.

Level 1 cloud amounts show field significance (at the 0.05 probability level) on day 1. There is a marked reduction (locally exceeding 0.3 or 30%) in the proportion of level 1 cloud, which has an overwhelming concentration over Antarctica (Figure 6a), in agreement with the zonally averaged results (Figure 5). There is no equivalent level 1 cloud feature over the northern polar region, where the highest clouds in substantial quantities are at level 4. Given the height of level 1 cloud it is possible that this represents polar stratospheric clouds (PSCs), which are thought to be thicker over Antarctica than the Arctic and thus produce a stronger signal in the thermal IR. The reduction of level 1 cloud over Antarctica is concentrated into the local winter months (not shown) when the absence of daylight precludes multispectral cloud type identification in ISCCP data. The other field significant cloud variable (at the 0.05 probability level) is level 4 cloud (440–560 mbar) at day -1 and day 2. Globally, level 4 cloud shows a decline through the FD period (Table 3). Although there is a good deal of local variability in cloud level 4 proportion anomalies, it is apparent that the largest reductions of up to 0.12 (12%) are concentrated into the high geomagnetic latitude regions of the Northern Hemisphere (Figure 6b) in line with the zonally averaged results (Figure 5).

Finally, the results of the analysis conducted on the FD-SP events show no significant changes in cloud proportion (even at the 0.1 probability level) for any cloud variable, at any spatial scale; neither globally (Table 4), over geomagnetic latitude bands, or spatially through field significance testing (results not shown). This occurs despite the far larger magnitude of reduction in GCR during FD-SP compared with FD events (Table 2).

4. Discussion

The question of how, and to what extent, the climate system may be influenced by solar-related variability remains central to our understanding of any anthropogenic effects on climate. The possible influence of variability in cosmic ray flux on cloud cover, and

thus the planet's radiation budget, has stimulated a lively debate within climate science in recent years. However, the effect on cloud of short-term variations in GCR associated with FD events has received little attention in the literature, in contrast to that at longer timescales of the 11-year solar cycle [e.g., *Svensmark and Friis-Christensen, 1997; Marsh and Svensmark, 2000*].

Indeed, it may be argued that FD events represent a relatively "pure" indicator of GCR variability in that there are no known natural internal modes of climate variability that operate with similar temporal characteristics. In addition, by distinguishing FD and FD-SP events we may be able to highlight the role of GCR relative to other effects of solar variability such as those identified by *Arnold and Robinson [1998], Bezprozvannaya et al. [1997], Brasseur and Solomon [1995], Gabis and Troshichev [2000], Haigh [1996, 1999], Labitzke and van Loon [1989, 1992], van Loon and Labitzke [1998], and Tinsley [2000]*. As such, the methodology adopted here may provide a useful way of separating the GCR signal from other possible external and internal influences on cloud cover.

In this study, we present the results of the most extensive assessment of the effects of short-term Forbush decreases of GCR on global cloud cover conducted to date. From the array of results a pattern emerges in those that are statistically significant. There is evidence of a statistically significant reduction (of up to 0.014 or 1.4%) in global-scale cloud proportion from 1 day prior to 1 day following the onset of FD events. However, it is of considerable importance to quantify the three-dimensional spatial structure of these cloud anomalies.

First, the effect is more pronounced over land surfaces (maximum of -0.034 at day 1) in comparison to oceans (maximum -0.005 ; not significant) and is a cumulative effect of reductions in the four uppermost cloud levels in the ISCCP D1 data. Second, zonally averaging data over geomagnetic latitude bands indicates that the decline is concentrated over polar geomagnetic latitudes, particularly of the Southern Hemisphere where large reductions (up to 0.18 or 18%) are observed throughout the FD period. This occurs largely in the proportion of the highest-level clouds in the each polar region. These decreases in high-latitude cloud are accompanied by a small increase in cloud at $\varphi = 30^\circ\text{N}$.

Finally, interpreting the gridded spatial pattern of cloud anomalies at 2.5° resolution is more problematic given the high level of cloud variability at this small scale associated with mesoscale, synoptic, and planetary-scale high-frequency atmospheric variability. Thus identifying the precise location (at the grid cell scale) of changes in total cloud amount cannot be achieved with a high degree of confidence. Nevertheless, we can be confident that the amount of cloud at the uppermost level in the polar regions declines in association with FD events. There are substantial (field significant) decreases in cloud level 1 proportion over Antarctica by up to 0.3 (30%) at day 1. This represents a notable new finding, particularly given the important role PSCs play in ozone chemistry [Tabazadeh *et al.*, 2000]. Field significant anomalies also occur in cloud level 4 at day -1 , where a decline is observed over the Northern Hemisphere polar region.

It is interesting to note that there are no significant anomalies associated with low-level cloud at any spatial scale. Nor are significant anomalies observed where ISCCP D1 data involved daytime observations. Thus we cannot identify significant anomalies associated with particular cloud types. However, it is quite possible that this is a result of larger errors in the multispectral satellite algorithms used to define cloud types, relative to those variables based on IR temperate thresholds only. Finally, there are no statistically significant anomalies observed for FD events associated with solar proton events.

Determining the physical mechanism(s) which cause the observed cloud anomalies is challenging, given the complexity of possible solar influences. However, the results, indicating that significant cloud anomalies are largely restricted to the highest-level cloud over the polar latitudes (particularly of the Southern Hemisphere) during FD events are in line with many theories describing the effect of GCR on cloud microphysics. These suggest that the polar regions experience the greatest penetration of GCR and that GCR induced ionization peaks in the upper troposphere and lower stratosphere, precisely where ISCCP level 1 cloud occurs. It is possible that the changes in cloud preceding the onset of FD events (by up to 1 day) may simply reflect the decline in GCR observed in the high geomagnetic latitude neutron monitor sites on average some 12 hours prior to 0000 UTC on the FD onset day. In addition, there is considerable dispersal within the composites of GCR such that some FD events involve small decreases in GCG a few days prior to FD onset.

However, the results do not support firm conclusions on the operation of any particular mechanism linking GCR and clouds given that the direct and indirect (via the electric circuit) effects may have a similar space/time structure. Nevertheless, the observed structure of cloud cover changes involving a small increase (large decrease) in cloud at $\varphi \sim 30^\circ\text{N}$ (polar latitudes) might be expected to result from cloud microphysical processes associated with a large-scale modulation of the global electric circuit, in which the air-Earth current density (and thus supply of electrostatic charge) is at its maximum (minimum) at low (high) latitudes during FD events [Tinsley, 1996]. In fact, Earth-atmosphere current density increases (statistically insignificant) have been observed over Mauna Loa, Hawaii ($\varphi = 20^\circ\text{N}$) around 4 days after FD events [Engfer and Tinsley, 1999]. Why there is no increase in cloud observed at subtropical latitudes of the Southern Hemisphere is not clear, although it may relate to the existence of the Southern Hemisphere convergence zones, which produce greater cloud cover in these latitudes compared with the Northern Hemisphere (by 12% at $\varphi = 30^\circ\text{N}$) such that any GCR/cloud microphysical processes are relatively less important. Indeed, it may be no coincidence that the increase in cloud proportion is observed at $\varphi = 30^\circ\text{N}$ where the global minimum in cloud proportion occurs (Figure 1).

That no significant cloud anomalies emerge for FD events associated with solar proton events, when the reduction in GCR is accompanied by an increase in SP flux, further suggests a

specific role of GCR in modulating cloud microphysics. The primary cause of FD events is solar coronal mass ejection, which is also associated with other potentially important solar phenomena, including increases in ultraviolet radiation (UV) and changes to stratospheric chemistry and the solar wind [Brosseur and Solomon, 1995; Herman and Goldberg, 1978]. Gabis and Troshichev [2000] observe increases in UV prior to and during FD and SP events, and they suggest this may result in perturbations in the large-scale stratospheric (and subsequently tropospheric) circulation. Changes in UV and stratospheric chemistry over the duration of the 11-year solar cycle have also been shown to result in substantial changes to the large-scale circulation of the lower atmosphere in GCM simulations [Haigh, 1996, 1999] and observations [van Loon and Labitzke, 1998]. Tinsley [2000] suggests that the current flow in the global electric circuit (and thus, potentially, cloud cover) can be modulated by relativistic electron precipitation from the magnetosphere and the ionospheric potential distribution in the polar cap regions, in addition to GCR modulation of ionospheric conductivity [Tinsley, 2000]. These former two processes are related to the strength of the solar wind, changes in which can precede the onset of FD events.

It is expected that changes in UV, stratospheric chemistry, and solar wind will occur during all FD events including those associated with SP events. In fact, UV anomalies are larger for SP than FD events [Gabis and Troshichev, 2000]. Thus the differing cloud response to FD and FD-SP events may preclude other mechanisms acting in isolation as an explanation of the results, and it suggests that the degree of cosmic ray ionization in the middle to lower atmosphere, (which may initiate direct or indirect effects (via the electric circuit) on cloud microphysical processes) could be a critical factor. Such a conclusion is tentative, however, given that we have not examined the other solar-related variables explicitly. Of course, it is always problematic to identify cause and effect from empirical studies, and it is plausible that a combination of mechanisms may explain the observations. This might involve the direct or indirect effect of GCR in conjunction with UV variability and/or other mechanisms which modulate the global electric circuit. However, any effect of these other processes on cloud has yet to be determined.

Finally, it is notable that the results presented here show very little similarity with the cloud cover changes at interannual timescales observed (and ascribed to GCR variability) by Svensmark and Friis-Christensen [1997], Marsh and Svensmark [2000], and Palle Bago and Butler [2000]. In those studies, positive correlations between interannual cloud cover and GCR are strongest for low-level cloud (on average 2 km) and over ocean surfaces of the tropics and midlatitudes. Here we find no significant anomalies in low-level cloudiness associated with short-term GCR variability. The disparities between those studies and the present work may simply represent the difference in timescales under study, such that the effect of GCR on low-level cloud is largely apparent over longer time periods than those associated with FD events. In addition, the mean FD in GCR is 4.7%, roughly 50% of the variation in GCR over an 11-year solar cycle. These disparities may prove important to our understanding of the likely mechanisms by which GCR may influence cloud. Alternatively, it may be that our results, based on a sample of GCR variability that excludes other mechanisms of internal and external climate variability, suggest that the correlation between interannual variability in GCR and low-level cloud observed in previous studies may not necessarily reflect a causal relationship.

5. Conclusions

This study presents interesting new findings on the possible effect of short-term changes in galactic cosmic ray flux associated with Forbush decrease events. The results indicate that overall, the

changes in cloud amounts associated with FD events are relatively small in magnitude and duration but have a highly specific spatial structure. Substantial reductions in the highest-level clouds are observed at polar latitudes immediately prior to and following FD events, particularly notable over Antarctica. Although this represents a small proportion of the globe, the effects on atmospheric chemistry and regional climate may be substantial and justifies further analysis. A small increase in total cloud is observed over Northern Hemisphere subtropical geomagnetic latitudes.

That there appears to be a latitude and height dependence of the cloud response to FD events is broadly consistent with some theories on GCR/cloud mechanisms. Consideration of the insignificant cloud changes during FD events associated with solar proton events suggests that the results are unlikely to be explained by other single mechanisms acting in isolation and provide additional circumstantial evidence of a GCR/cloud relationship. However, the complexity of solar influences on the atmosphere should not be understated and the results do not support any firm conclusion on the mechanism by which GCR may influence clouds. Our results do not concur with some previous empirical work on GCR/cloud relations suggesting that the mechanisms and potential effects on climate may be more complex than previously stated. However, it must be borne in mind that this study is concerned only with short-term changes in GCR. Empirical results such as these cannot prove any theory on the mechanisms by which GCR may influence cloud, and the work emphasizes the need for further research into this topic.

In keeping with all empirical studies of this kind there are a number of caveats that must be noted when interpreting the results. First, given the complexity of solar-atmosphere relations there remain other possible physical explanations of observed changes in cloud. Other mechanisms related to solar variability include the direct effect of the solar wind or solar UV radiation. Although the comparison of the FD and FD-SP samples should account for many of these further research is necessary to test competing hypotheses.

Second, it is possible that the satellite instruments that supply the data and/or the algorithms used to extract cloud information, are not sufficiently sensitive or accurate, respectively, such that data errors are large relative to any physical GCR/cloud signal. This is a possible explanation of the absence of significant cloud anomalies for variables incorporating visible data, where errors are likely to be higher than those associated with the IR channel only. In addition, for numerous reasons, satellite cloud retrievals are most problematic over polar regions under nighttime/wintertime conditions [Rossow and Schiffer, 1999] where we identify the most significant changes in cloud proportion. However, we feel it is unlikely that satellite errors are responsible for our results given the relatively "random" nature of the FD sampling and the results of the Monte Carlo simulations using an extensive ISCCP D1 database. It is also possible that because the satellites cannot quantify multilayered cloud, the cloud amounts at different vertical levels are not truly independent of each other in that low-level cloud amounts may be inversely related to those at upper levels. This might mask a real decline in low-level clouds during FD events.

Third, the study is based on data from a relatively short period such that our sample of FD events is smaller than some previous studies, which have utilized longer-term surface-based meteorological observations. While a short data set is more sensitive to random data anomalies, we must wait for a number of years before the satellite database will be extended substantially. Finally, by assuming linearity and uniformity in the response of the atmosphere to FD events the methodology of epoch superposition itself may conceal important information on the precise nature of these interactions. Analysis of individual FD events may well prove a fruitful avenue for further research but is beyond the scope of this paper.

Acknowledgments. The authors would like to thank the International Satellite Cloud Climatology Program (ISCCP) and the Goddard Institute for

Space Studies for production of the ISCCP data and the Distributed Active Archive Center at Langley Research Center, EOSDIS, for its distribution. These activities are sponsored by NASA's Mission to Planet Earth. We are also grateful to the NOAA National Geophysical Data Center for data on Forbush decreases in cosmic ray flux. Hourly neutron monitor data were obtained from the Space Physics Data System of the University of Chicago (funded by National Science Foundation grant ATM-9912341).

References

- Arnold, N. F., and T. R. Robinson, Solar cycle changes to planetary wave propagation and their influence on the middle atmosphere circulation, *Ann. Geophys.*, **16**, 69–76, 1998.
- Bezprozvannaya, A. S., G. I. Ohl, B. I. Sazonov, A. Scherba, T. I. Schuka, and O. A. Troshichev, Influence of short-term changes in solar activity on baric field perturbations in the stratosphere, *J. Atmos. Sol. Terr. Phys.*, **59**, 1233–1244, 1997.
- Brasseur, G., and S. Solomon, *Aeronomy of the Middle Atmosphere*, 447 pp., D. Reidel, Norwell, Mass., 1995.
- Dickinson, R. E., Solar variability and the lower atmosphere, *Bull. Am. Meteorol. Soc.*, **56**, 1240–1248, 1975.
- Engfer, D. W., and B. A. Tinsley, An investigation of short-term solar wind modulation of atmospheric electricity at Mauna Loa observatory, *J. Atmos. Sol. Terr. Phys.*, **61**, 943–953, 1999.
- Farrar, P. D., Are cosmic rays influencing oceanic cloud coverage: Or is it only El Niño?, *Clim. Change*, **47**, 7–15, 2000.
- Feynman, J., and A. Ruzmaikin, Modulation of cosmic ray precipitation related to climate, *Geophys. Res. Lett.*, **26**, 2057–2060, 1999.
- Gabis, I. P., and O. A. Troshichev, Influence of short-term changes in solar activity on baric field perturbations in the stratosphere and troposphere, *J. Atmos. Sol. Terr. Phys.*, **62**, 725–735, 2000.
- Haigh, J. D., The impact of solar variability on climate, *Science*, **272**, 981–984, 1996.
- Haigh, J. D., A GCM study of climate change in response to the 11-year solar cycle, *Q. J. R. Meteorol. Soc.*, **125**, 871–892, 1999.
- Herman, J. R., and R. A. Goldberg, Sun, weather, and climate, *NASA Spec. Publ.*, **SP 426**, 320 pp., 1978.
- Jorgensen, T. S., and A. W. Hansen, Comments on "Variation of cosmic ray flux and global cloud coverage: A missing link in solar-climate relationships," by Henrik Svensmark and Eigil Friis-Christensen, *J. Atmos. Sol. Terr. Phys.*, **62**, 73–77, 2000.
- Kernthaler, S. C., R. Toumi, and J. Haigh, Some doubts concerning a link between cosmic ray fluxes and global cloudiness, *Geophys. Res. Lett.*, **26**, 863–865, 1999.
- Kristjansson, J. E., and J. Kristiansen, Is there a cosmic ray signal in recent variations in global cloudiness and cloud radiative forcing?, *J. Geophys. Res.*, **105**, 11,851–11,863, 2000.
- Krivsky, L., and B. Ruzickova-Topolova, Parameters of Forbush decreases and their parent flares in the solar cycle 1965–1976, *Bull. Astron. Inst. Czech.*, **29**, 30–44, 1978.
- Labitze, K., and H. van Loon, Association between the 11 year solar cycle, the QBO and the atmosphere, part III, Aspects of the association, *J. Clim.*, **2**, 554–565, 1989.
- Labitze, K., and H. van Loon, Association between the 11 year solar cycle and the atmosphere, part V: Summer, *J. Clim.*, **5**, 240–251, 1992.
- Lassen, K., and E. Friis-Christensen, Variability of the solar cycle length during the past five centuries and the apparent association with terrestrial climate, *J. Atmos. Terr. Phys.*, **57**, 835–845, 1995.
- Livezey, B. C., and W. Y. Chen, Statistical field significance and its determination by Monte Carlo techniques, *Mon. Weather Rev.*, **111**, 46–59, 1983.
- Marsh, N., and H. Svensmark, Low cloud properties influenced by cosmic rays, *Phys. Rev. Lett.*, **85**, 5004–5007, 2000.
- Mason, S. J., and P. D. Tyson, The modulation of sea-surface temperature and rainfall associations over southern Africa with solar-activity and the quasi-biennial oscillation, *J. Geophys. Res.*, **97**, 5847–5856, 1992.
- Palle Bago, E., and C. J. Butler, The influence of cosmic rays on terrestrial clouds and global warming, *Astron. Geophys.*, **41**, 4.18–4.22, 2000.
- Pruppacher, H. R., and J. D. Klett, *Microphysics of Clouds and Precipitation*, 954 pp., Kluwer Acad., Norwell, Mass., 1997.
- Pudovkin, M. I., and S. V. Veretenenko, Cloudiness decreases associated with Forbush-decreases of galactic cosmic rays, *J. Atmos. Sol. Terr. Phys.*, **57**, 1349–1355, 1995.
- Ramanathan, V., R. D. Cess, E. F. Harrison, P. Minnis, B. R. Barkstrom, E. Ahmad, and D. Hartmann, Cloud-radiative forcing and climate: Results from the Earth Radiation Budget Experiment, *Science*, **243**, 57–63, 1989.
- Reiter, R., *Phenomena in Atmospheric and Environmental Electricity*, 541 pp., Elsevier Sci., New York, 1992.

- Rossow, W. B., and R. A. Schiffer, Advances in understanding of clouds from ISCCP, *Bull. Am Meteorol Soc.*, *80*, 2261–2287, 1999.
- Rossow, W. B., A. W. Walker, D. E. Beuschel, and M. D. Roiter, ISCCP documentation of new cloud datasets, *WMO Tech. Doc. 737*, 115 pp., World Clim. Res. Program, Geneva, Switzerland, 1996.
- Svensmark, H., and E. Friis-Christensen, Variation of cosmic ray flux and global cloud coverage: A missing link in solar-climate relationships, *J Atmos Sol Terr. Phys.*, *59*, 1225–1232, 1997.
- Tabazadeh, A., M. L. Santee, M. Y. Danilin, H. C. Pumphrey, P. A. Newman, P. J. Hamill, and J. L. Mergenthaler, Quantifying denitrification and its effect on ozone recovery, *Science*, *288*, 1407–1411, 2000.
- Tinsley, B. A., Correlations of atmospheric dynamics with solar wind-induced changes of air-earth current density into cloud tops, *J. Geophys Res.*, *101*, 29,701–29,714, 1996.
- Tinsley, B. A., Influence of solar wind on the global electric circuit, *Space Sci. Rev.*, *94*, 258–321, 2000.
- Tinsley, B. A., and G. W. Deen, Apparent tropospheric response to MeV-GeV particle flux variations: A connection via electrofreezing of supercooled water in high level clouds?, *J. Geophys. Res.*, *96*, 22,283–22,296, 1991.
- Tinsley, B. A., and R. A. Heelis, Correlations of atmospheric dynamics with solar activity: Evidence for a connection via the solar wind, atmospheric electricity, and cloud microphysics, *J. Geophys Res.*, *98*, 10,375–10,379, 1993.
- Tinsley, B. A., G. M. Brown, and P. H. Scherrer, Solar variability influences on weather and climate: Possible connections through cosmic ray fluxes and storm intensification, *J. Geophys. Res.*, *94*, 14,783–14,792, 1989.
- Tinsley, B. A., R. P. Rohrbaugh, M. Hei, and K. V. Beard, Effects of image charges on the scavenging of aerosol particles by cloud droplets and on droplet charging and possible ice nucleation processes, *J. Atmos. Sci.*, *57*, 2118–2134, 2000.
- van Loon, H., and K. Labitzke, The global range of the stratospheric decadal wave, part I, Its association with the sunspot cycle in summer and in the annual mean, and with the troposphere, *J. Clm.*, *11*, 1529–1537, 1998.
- Yamada, Y., S. Yanagita, and T. Tshida, A stochastic model of the solar modulation phenomena of cosmic rays, *Geophys. Res. Lett.*, *25*, 2353–2356, 1998.

D. R. Kniveton, School of Chemistry, Physics and Environmental Science, University of Sussex, Falmer, Brighton BN1 9QJ, England, UK. (d.r.kniveton@sussex.ac.uk)

M. C. Todd, Department of Geography, University College London (UCL), 26 Bedford Way, London WC1H 0AP, England, UK. (m.todd@geog.ucl.ac.uk)

(Received January 25, 2001; revised June 19, 2001; accepted July 3, 2001.)